JOURNAL OF MATERIALS SCIENCE 24 (1989) 1719–1724

Au/P polysilicon Schottky diodes

P. CALEB DHANASEKARAN, K. R. MURALI, B. S. V. GOPALAM
Department of Physics, Indian Institute of Technology, Madras 600 036, India

Schottky barrier diodes were fabricated by evaporation of gold layers onto chemically etched polycrystalline silicon wafers. The wafers are p type (resistivity $\varrho_{\perp}$ = 160 Ωcm, the grains are columnar shape with some orientation). An average potential barrier of 0.087 eV appears to exist across the grain boundary between columns. Ohmic back contacts were made from a Ga–Al alloy. Diodes were investigated with the aid of (a) *I–V* characteristics at different temperatures, (b) *C–V* characteristics, (c) spectral response and (d) Fowler's plot of photoelectric measurements. The best diodes had characteristics similar to data typical of monocrystalline silicon. The low series columnar resistance (0.67 Ω) of the cells is neglected in the analysis. The barrier height, from *I–V* data (including temperature variation) was 0.67 to 0.73 eV. This is much lower than that obtained from Fowler's plot (0.9 eV). However, the barrier height obtained from the *C–V* graph is in agreement with the value of 0.9 eV. The diffusion potential is 0.4 eV. The value of the diode ideality factor (1.5 to 2.8) indicates that recombination generation processes play a dominant role. The normalized photovoltaic spectral response in the wavelength range 600 to 1300 nm was presented with a comparison from the theory taking into account bulk and surface recombination.

1. Introduction

Schottky barrier diodes [1] were the first semiconductor devices to be studied. They are really metal–semiconductor contacts in ideal terms. The barrier should be abrupt. In this way, the contact between a metal and a semiconductor element or compound forms a potential barrier and thus leads to rectification. Crowell and Sze [2] studied the contacts between gold and silicon and gold and GaAs. Recently the metal contacts on ternary and quaternary semiconductors have also been studied. Even then due to contamination of the surface, the surface effects and mechanical defects, the analysis of the experiments on Schottky barrier diodes becomes complicated. However these devices are very useful as solar cells. In the following a gold–polycrystalline silicon (p) Schottky barrier is analysed.

2. Fabrication

Small pieces of polysilicon were cut from 10 cm × 10 cm samples of 0.4 mm thick material to enable fabrication of diodes with an area of typically $\approx 0.3\,cm^2$. The wafers were well polished with 4 μm paper, followed by 0.4 μm grain size diamond paste. The samples were cleaned with ethyl alcohol to remove organic residues and then etched with CP6 [3]. They were carefully stored and protected from atmospheric contamination in vacuum desiccators. Whenever a Schottky diode is fabricated, a disc is taken out and cleaned well with isopropyl alcohol [4]. These were then coated with a 20 to 40 nm thick gold layer at a pressure of 10^{-6} torr. The back ohmic contact was made by applying Ga–Al paint which forms a low melting point alloy. The surface of the virgin silicon wafer is displayed by a photomicrograph as shown in Fig. 1a. It consists of columnar single crystallites having some slight preferred orientation. The average grain size corresponds to approximately 100 grains cm^{-2}. The conductivity type was tested using a hot probe technique, and found to be p type [5].

The type of contact formed with Ga–Al paint was tested with a curve tracer. In a separate experiment Ga–Al contacts were made to both sides of the wafer. Its resistivity was determined through *I–V* characteristics as shown in Fig. 1b. This was repeated at various temperatures. It showed a departure from ohmicity at temperatures below that of liquid nitrogen. For the temperature region under study the contacts showed a reliable ohmic nature, compared to Nicolex and other contacts. The formation of the barrier between gold and the polysilicon was checked by curve tracer and displayed in Fig. 2. Sometimes the ambient temperature

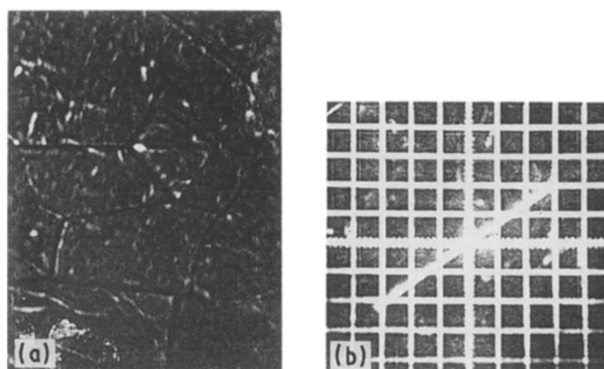

Figure 1 (a) Silicon wafer (×20), (b) ohmic contact.

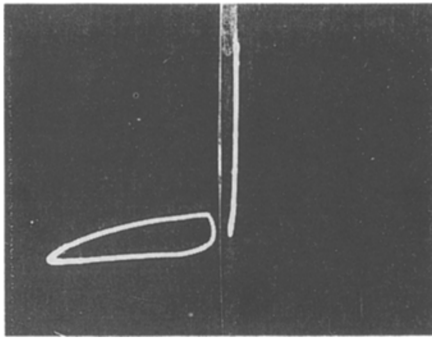

Figure 2 *I–V* characteristics (curve tracer) of a typical diode.

at which the contact is formed affects the formation. In some cases a little annealing is necessary.

3. Experiments

3.1. Conductivity variation with temperature

The resistivity of the material at room temperature was 160 Ωcm. The plot of conductivity against $1/T$ as shown in Fig. 3 shows two straight lines. The upper portion at high temperatures gives an activation energy $\Delta E = 0.41$ to 0.44 eV in the relation $\sigma = \sigma_0 \exp(-\Delta E/kT)$ describing the temperature variation of conductivity. The lower portion also can be fitted with a simple relation like the above yielding the activation energy in this case to be $\Delta E = 0.087$ eV. The former one can be identified as the depth of the trap from the top of the valence band. It lies close to the Fermi level. The second one is the potential hill due to a grain boundary.

3.2. Current density (i)–voltage (V) characteristics of the diode

As many as 100 diodes were tested and analysed with the help of *I–V* characteristics. These can be grouped into three main categories given by curves (a), (b) and (c) in Fig. 4. Sample C is adjudged to be a well behaved one both from *I–V* and *C–V* characteristics. The diodes are made of a sandwich type in a direction perpendicular to the plane of the wafer and along the columnar length. As such the series resistance of the diodes is of the order of 0.67 Ω. The effect of the series resistance throughout the analysis of these diodes is thus neglected. A more detailed display for the forward characteristics is shown in Fig. 5 as a semi-log plot. The semi-empirical formula for the forward characteristics is given by [6]

$$J = J_0[\exp(qV/AkT) - 1] \quad (1)$$

where A is the ideality factor, J_0 the saturation current density, V the forward voltage acting on the barrier, k the Boltzmann constant, T the temperature of the specimen in Kelvin, q the electronic charge, J the actual current density ($= I/S$), S the area of the diode, and I the current through the diode. The one in the brackets can be neglected, compared to the exponential

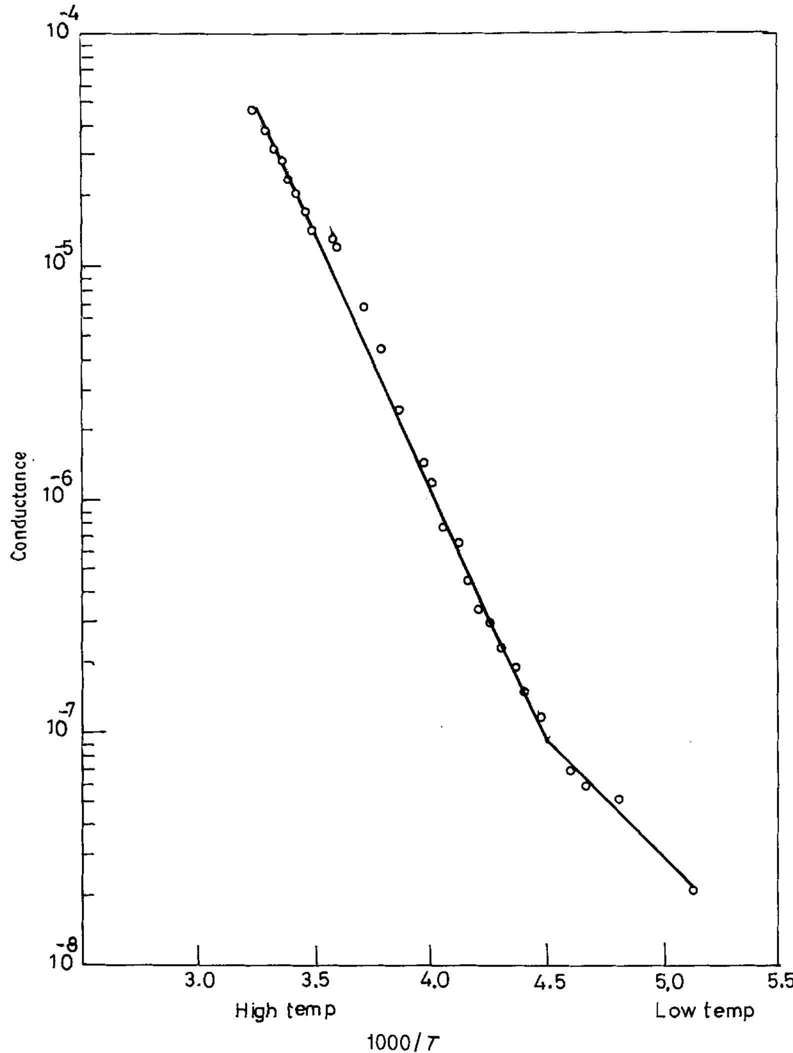

Figure 3 Conductance plotted against temperature.

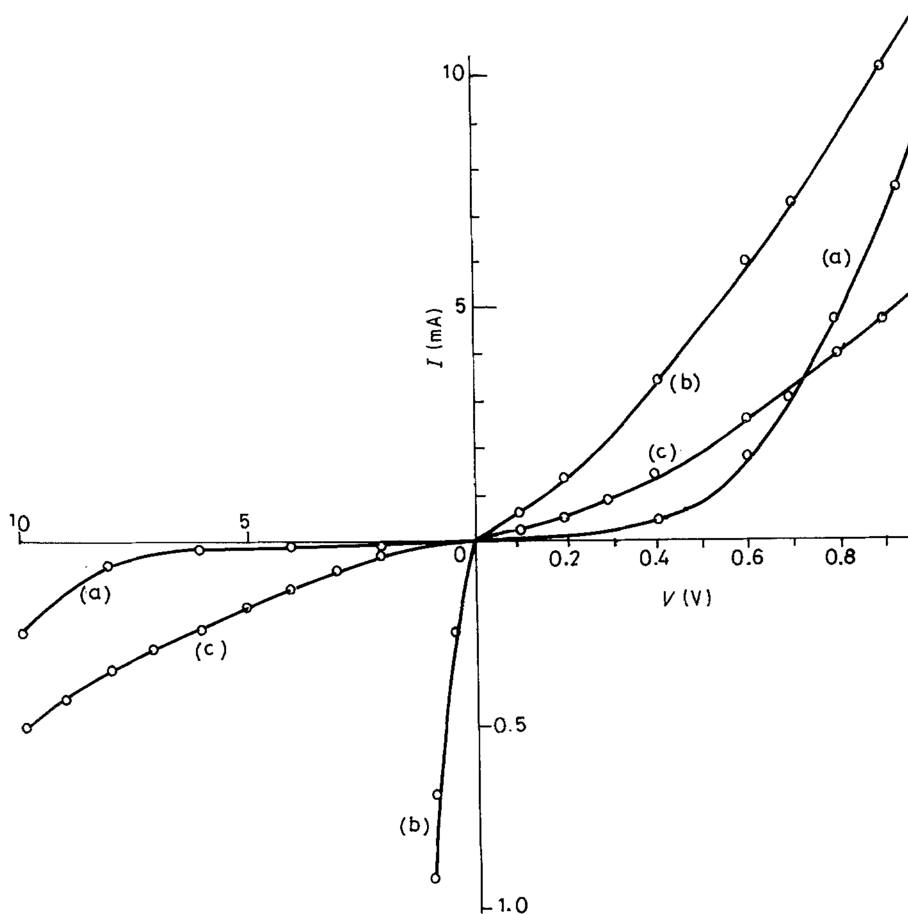

Figure 4 Current–voltage characteristic (gold–polysilicon–GaAl paint) (a) 0.6 V, (b) 0.2 V, (c) 0.4 V.

factor in the range of the forward voltages higher than kT/q if the effect of series resistance is negligible. The resulting equation can be written in the form

$$\ln J = \ln J_0 + qV/AkT \quad (2)$$

The reverse characteristics are shown in Fig. 6 as a semi-log plot. There are at least two clear regions: (a) a linear region for small voltages and (b) a region showing a tendency towards saturation but with some increase of current with voltage. This could have been due to several reasons such as (i) a volume generated current, (ii) dominance of the emission, (iii) affect of generation – recombination current etc. At still higher voltages the current tends to increase more sharply with bias due to avalanche breakdown. These characteristics yield the saturation current density as 30 to 33 $\mu A\,cm^{-2}$. The diode quality factor is found to lie between 1.5 to 2.8 for a typical sample like C. For the same sample the forward and reverse characteristics are observed with varying sample temperatures. These are shown as semi-log plots in Figs 7 and 8 respectively. An Arrhenius plot of ln (J_0/T^2) against $1/T$ is shown in Fig. 9. This is a straight line whose slope gives the metal–semiconductor work function. The value lies between 0.67 and 0.73 eV. The estimated values from both the forward and reverse characteristics agree fairly well with each other.

3.3. C–V measurement

The capacitance of the reverse biased diode was

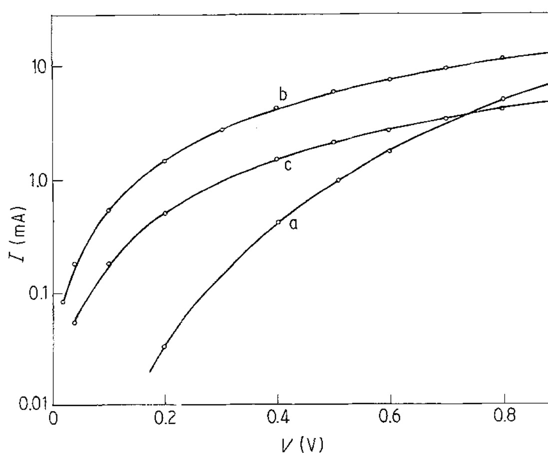

Figure 5 Forward bias: current–voltage characteristic (gold–polysilicon–GaAl paint). (a) $A = 2.8$, (b) $A = 2$, (c) $A = 1.52$.

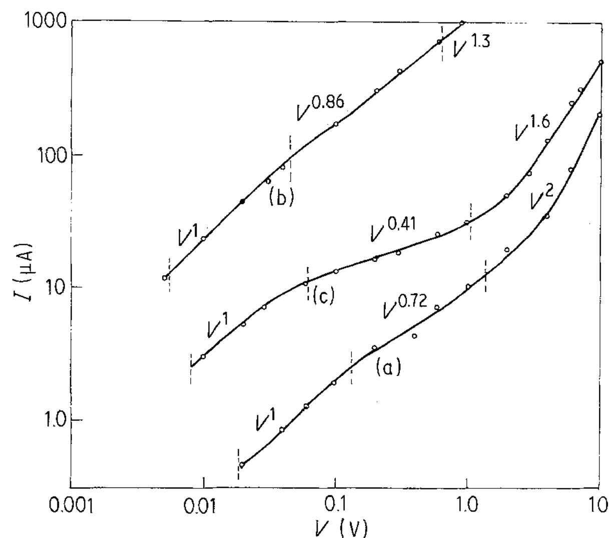

Figure 6 Reverse bias: current–voltage characteristic (gold–polysilicon–GaAl paint).

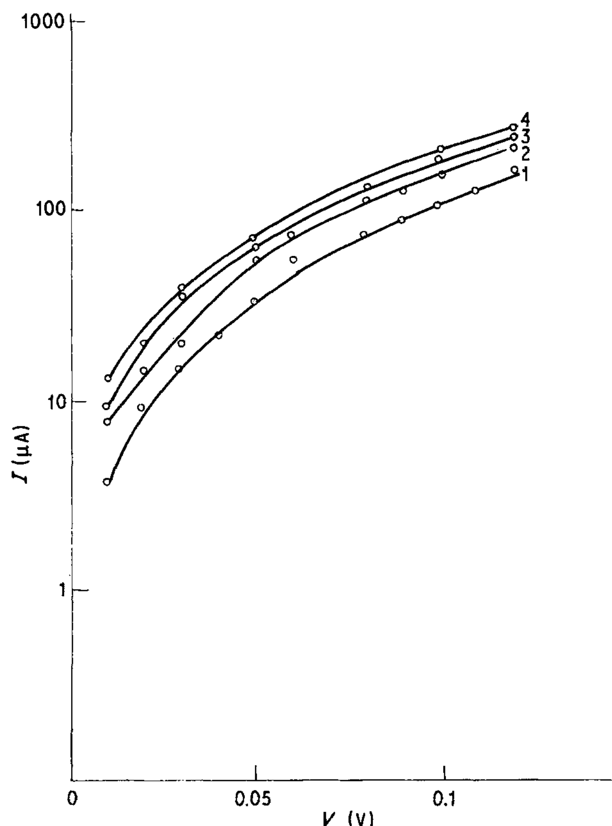

Figure 7 Current-voltage characteristics–temperature dependence (forward bias (40–120 mV) (gold-polysilicon–GaAl paint) (1 300 K, 2 308 K, 3 315 K, 4 326 K).

measured by *LCR* bridge. The graph in Fig. 10 is drawn with $1/C^2$ against the applied reverse bias V. This gives a straight line. The relationship for an ideal Schottky barrier is given by [7]

$$1/C^2 = \frac{2(V_D - V)}{S^2 q \varepsilon \varepsilon_0 N_A} \quad (3)$$

$$\frac{d(S^2/C^2)}{dV} = -2/\varepsilon \varepsilon_0 N_A \quad (4)$$

where ε_0 is the dielectric permittivity of vacuum, ε the

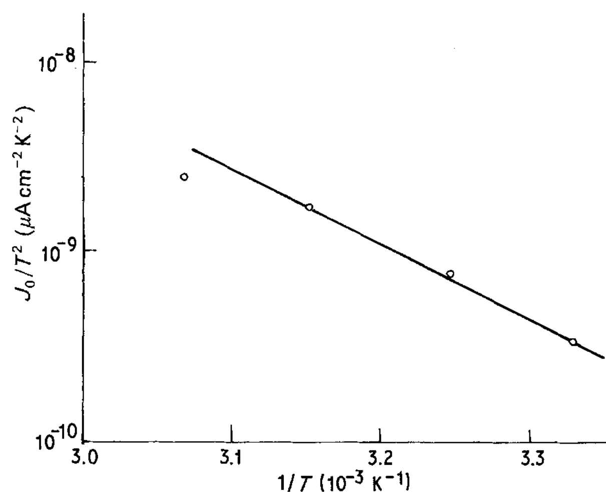

Figure 9 Gold-polysilicon-GaAl ln (J_0/T^2) against $1/T$ plot. Determination of barrier height from the temperature variation of J_0. The saturation current for both the forward and reverse characteristics are close (agreeing values are plotted).

dielectric constant of silicon, N_A the acceptor concentration, and V_D the diffusion potential.

The diffusion potential is close to 0.4 eV. The acceptor concentration is 1.2×10^{14} cm^{-3}. This agrees well with the resistivity of the flake in a direction perpendicular to its plane, as 160 Ωcm. The resistivity along the plane of the sample is only 5 Ωcm confirming the existence of the grain boundary barrier of 0.087 eV. The results of diffusion potential and work function give the separation of the Fermi level from the top of the valence band, as 0.27 eV. The *C–V* relationship is also a good measure of the degree of formation of the Schottky barrier. The *C–V* plot on a log–log scale is shown in Fig. 11 for the barriers "a" and "C". Diode "C" appears to be the one close to ideal Schottky behaviour. Schottky barrier "a" exhibits a linear gradient of impurity density, whereas the Schottky barrier will have only abrupt change in the impurity density. A summary of the results from the *I–V* and *C–V* characteristics is shown in Table I. + and − refer to forward and reverse characteristics, l, m and p are the exponents appearing in the three

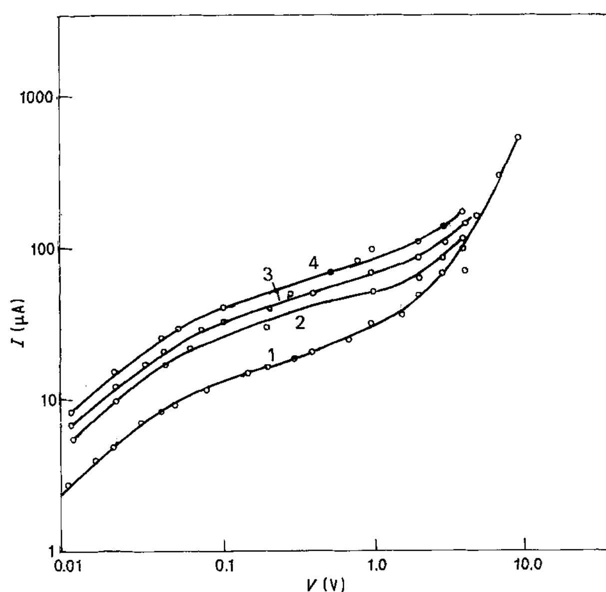

Figure 8 Reverse characteristics: temperature dependence (gold–polysilicon–GaAl paint).

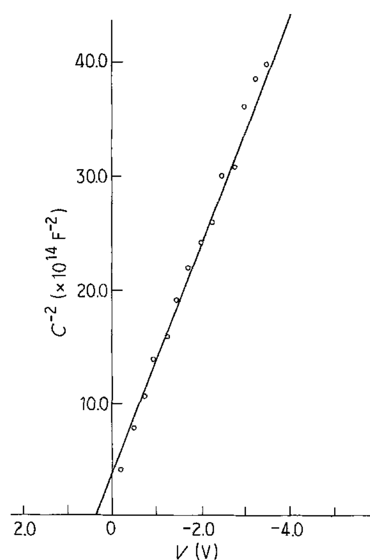

Figure 10 Variation of capacitance with reverse bias (Au–polysilicon–GaAl) $1/C^2$–V plot (gold positive) determination of V_d.

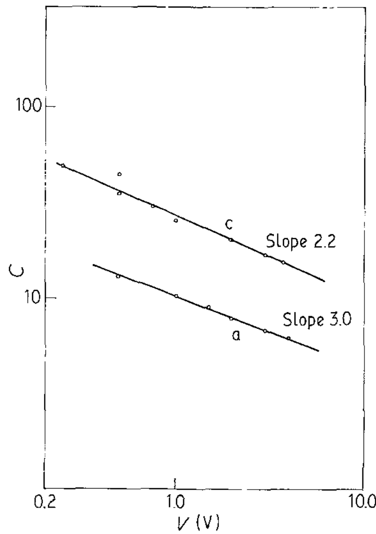

Figure 11 (Au–polysilicon–GaAl) ln C–ln V relationship. Testing formation of Schottky barrier (proves case c is a better Schottky diode).

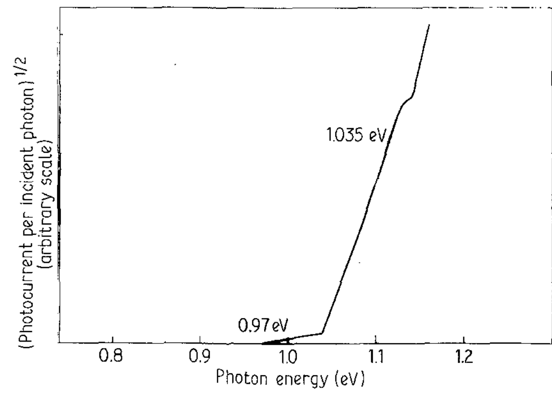

Figure 12 Fowler plot.

portions of Fig. 6, V_d is the diffusion potential, and ϕ the metal–semiconductor work function.

4. Photoelectric method

This is another interesting technique to determine the metal–semiconductor barrier height. The Fowler plot, as shown in Fig. 12, a graph of the square root of the relative photoresponse plotted against photon energy in general gives a straight line. The intercept of this straight line on the photon axis gives the metal–semiconductor work function. This turns out to be 0.97 eV. This is higher than that obtained from the I–V characteristics. This is mostly true as $T^{3/2}$ variation is small compared to the exponential relation of the density of electrons function. As such the I–V characteristics usually give a lower barrier height.

5. Spectral sensitivity of the photocell

In order to study the photoresponse of the cell for its potential use as a photocell, another experiment namely spectral response of the cell in the range of wavelengths 500 nm to 1300 nm was performed. The normalized photoresponse is plotted with respect to the wavelength in Fig. 13. This gives a smooth symmetric curve with a maximum near 935 nm. The photoresponse current can be treated as the sum of three components (i) hole diffusion current in the inversion n-layer (width x_i) (ii) the hole–electron generation current resulting from the excitation by photons and (iii) recombination–diffusion electron current in the bulk p region (of width w) beyond the depletion layer. The constants obtained by computer simulation are given by $w = 5\,\mu$m, $x_i = 3\,\mu$m, $L_n = L_p = 1100\,\mu$m = minority carrier diffusion lengths, $S_p = 100\,\text{m sec}^{-1}$ = surface trap, no recombination velocity.

6. Discussion

The equation of the diode given earlier consists of

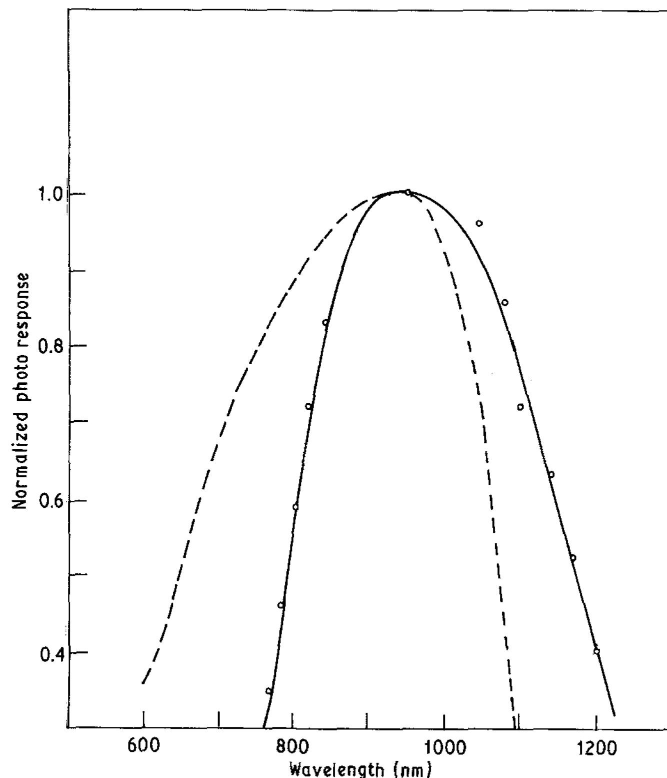

Figure 13 Photovoltaic spectrum comparison between experiment (——) and theory (- - -): polycrystalline Si–gold Schottky barrier diode. $W = 5\,\mu$m, $X_I = 3\,\mu$m, $L_n = L_p = 1.1 \times 10^{-4}$ m, $D_n = 0.36 \times 10^{-2}\,\text{m}^2\,\text{sec}^{-1}$, $D_p = 0.15 \times 10^{-12}\,\text{m}^2\,\text{sec}^{-1}$, $S_p = 100\,\text{m sec}^{-1}$.

TABLE I Parameters obtained from I–V and C–V characteristics

	a	b	c
$J_0(\ )$ (μA cm^{-2})	13.0	–	57.0
$J_0(+1)$ (μA cm^{-2})	15.0	10.0	53.0
$J(0)$ (μA cm^{-2})	23.5	63.1	32.0
$\phi(+)$ (eV)	0.71	0.71	0.67
$\phi(-)$ (eV)	0.71	–	0.67
$\phi(0)$ (eV)	0.69	0.67	0.69
V_d (I–V) (eV)	0.60	0.20	0.40
V_d (C–V) (eV)	0.42	0.32	0.39
A	2.8	2.00	1.52
l	1.00	1.00	1.00
m	0.72	0.86	0.42
P	2.00	1.30	1.6

the saturation current density J_0. There are two models to explain this saturation current density in the literature namely (a) approximate junction model and (b) modified model given by Crowell and Beguwala and Williams. According to these

$$J_0 = J_{th} G(\tau) \quad \text{Model (a)} \tag{5}$$

$$J_0 = J_{th} H(\tau) \quad \text{Model (b)} \tag{6}$$

$$J_{th} = N_v q \cdot \bar{v} \exp(-q\phi/kT) \tag{7}$$

where $N_v = P = 1.2 \times 10^{20}\,\mathrm{m}^{-2}$ = density of holes, $\bar{v} = 1.17 \times 10^5\,\mathrm{m\,sec^{-1}}$ = average thermal velocity of holes and

$$\phi = 0.9\,\mathrm{eV} \text{ (on an average)}$$

$$J_{th} = 5.2 \times 10^{-10}\,\mathrm{A\,m^{-2}}$$

$$G(\tau) = 2.5(\tau_R)^{1/2}\tau^{-1/2} \tag{8}$$

where τ_R = relaxation time of the holes and τ = effective recombination lifetime

$$\tau_R = 10^{-12}\,\mathrm{sec}$$

$$G(\tau) = 2.5 \times 10^{-5}\,\tau^{-1/2}$$

and $H(\tau)$ is given by

$$H(\tau) = \left(\frac{L\mu F_s}{\bar{v}_2}\right)^{1/2} \tau^{-1/2} \tag{9}$$

where

$$\mu = 600 \times 10^{-4}\,\mathrm{m^2\,V^{-1}\,sec^{-1}}$$

$$F_s = \text{surface electric field} = 10^6\,\mathrm{V\,m^{-1}}$$

$$H(\tau) = 2.1 \times 10^{-5}\,\tau^{-1/2} \tag{10}$$

and

$$L = \text{effective diffusion length} = 100\,\mu\mathrm{m}.$$

The lifetime calculated from the expressions of J is very small and is of the order of nanoseconds, for a saturation current density of $10\,\mu\mathrm{A\,cm^{-2}}$, model (a) gives 1.7×10^{-10} sec while (b) gives 1.2×10^{-10} sec. These results indicate the theory for Schottky barriers made up of polysilicon substrates with large areas needs to be modified from many points of view.

7. Summary

Boron-doped p type polycrystalline–gold Schottky barrier diodes are fabricated. They are characterized by (a) I–V characteristics (b) C–V characteristics (c) Fowler plot and (d) by spectral sensitivity characteristics. The values of diffusion potential ideality factor, metal–semiconductor work function, equilibrium hole density, and the approximate lifetime are estimated. Some discrepancies which arose between the theoretical models and the experimental results are listed.

References

1. W. SCHOTTKY, *Natur. Wiss.* **26** (1938) 843.
2. C. R. CROWELL and S. M. SZE, *J. Appl. Phys.* **37** (1966) 2683.
3. V. A. BRUK, V. V. GARSHENIN and A. I. KURNOSOV, "Semiconductor Technology" (Mir Publishers, Moscow, 1969).
4. W. R. RUNYAN, "Semiconductor Measurements and Instrumentation" (McGraw Hill, Dallas, Texas, 1975).
5. W. CRAWFORD DUNLAP Jr, "An Introduction to Semiconductors" (Wiley, New York, 1975).
6. EBERHARD SPENKE, "Electronic Semiconductors" (McGraw Hill, New York, 1958).
7. S. M. SZE, "Physics of Semiconductor Devices" (Wiley Eastern Ltd, New Delhi, 1969) Ch. 8.

Received 11 January and accepted 25 May 1988